PALEOCEANOGRAPHY, VOL. 15, NO. 5, PAGES 551-563, OCTOBER 2000

Intercomparison of coral oxygen isotope data and historical sea surface temperature (SST): Potential for coral-based SST field reconstructions

Michael N. Evans,[1] Alexey Kaplan, and Mark A. Cane[2]
Lamont-Doherty Earth Observatory, Palisades, New York

Abstract. We examine the extent to which the large-scale features of the sea surface temperature (SST) anomaly field are represented by a sparse observational network of coral oxygen isotope (δ^{18}O) time series. Regression of annually averaged δ^{18}O data against gridded estimates of local SST anomaly within the period 1856–1990 confirm the literature regression of δ^{18}O anomaly on SST anomaly for Indo-Pacific corals. However, while interannual SST variability is generally well represented by individual coral time series, observed decadal and secular variability does not always display a linear relationship to local SST anomaly. Instead, many records appear to better recover nonlocal, large-scale phenomena, which in turn are related to either the coral local SST or SST covariant changes in seawater δ^{18}O. We employ empirical orthogonal function (EOF) analysis to identify common patterns of variability in the coral data. We find two significant patterns which are interpretable as the oceanographic signature of the El Niño-Southern Oscillation (ENSO) and as a near-global warming in which the eastern equatorial Pacific cools. A third pattern weakly resembles the Pacific Decadal Oscillation. These modes are seen more clearly in a singular vector decomposition (SVD) of the covariance between the coral data and the dominant patterns of large-scale historical SST variability. The results are consistent with those found in EOF and SVD analyses of SST data from the coral locations. As additional coral-based proxy estimates become available, they will improve the resolution of the patterns recovered. These results suggest that a sparse network of coral data may be used to reconstruct interannual, secular, and decadal SST variability for preinstrumental periods, albeit with large uncertainty.

1. Introduction

Much work in the rapidly growing field of coral paleoclimatology has emphasized the need to put secular climatic trends, shifts, and decadal variability observed in the instrumental record within the context of longer-term reconstructions of natural variability [*Dunbar and Cole*, 1993; *Martinson et al.*, 1995]. Toward this goal many coral-based proxy time series have been calibrated and interpreted not only in terms of local conditions but also as monitors of the low-frequency variability of large-scale spatial patterns of near-surface atmospheric and/or oceanographic phenomena [*Cole and Fairbanks*, 1990; *Cole et al.*, 1993; *Druffel and Griffin*, 1993; *Quinn et al.*, 1993, 1998; *Linsley et al.*, 1994; *Dunbar et al.*, 1994; *Tudhope et al.*, 1995; *Charles et al.*, 1997; *Moore and Charles*, 1998; *Evans et al.*, 1998a, 1999]. The success of these studies suggests the potential for what we term a climate field reconstruction (CFR) from the coral-based proxy data [*Evans et al.*, 2000]: a spatiotemporal estimate of some climatic variable of interest, optimally based on all available observations, extending from the present into the preinstrumental period, and with quantified uncertainty. On the basis of available data and research in progress in a number of laboratories worldwide, it may soon be possible to reconstruct sea surface temperature (SST) fields from coral δ^{18}O data for the past three to four centuries.

However, it has been suggested that at least some of the low-frequency variability observed in proxy data may not be directly attributable to climate variability [*Jones et al.*, 1998]. In particular, *Crowley et al.* [1999] found that decadal and secular variability in five coral δ^{18}O records was significantly larger than the local and gridded historical observations would indicate and attributed the discrepancy to instability of the regression of SST on δ^{18}O. Hence a prerequisite for CFR is the calibration or validation of the proxy data in terms of the climate field and over the timescales to be reconstructed [*Quinn et al.*, 1998; *Crowley et al.*, 1999; *Evans et al.*, 2000].

[1]Now at Department of Earth and Planetary Sciences, Harvard University, Cambridge, Massachusetts.

[2]Also at Department of Earth and Environmental Sciences, Columbia University, New York, New York.

Paper number 2000PA000498.
0883-8305/00/2000PA000498$12.00

Shy of an actual reconstruction attempt, we focus here on the intercomparison of coral oxygen isotope (δ^{18}O) data and historical observations of SST anomaly. Potential biases in a coral-based estimate of SST variability (additional climatic influences, local proxy calibration and age model uncertainties, and sampling artifacts) should be independent of those in the instrumental record (instrument calibration, precision, accuracy, measurement method, data scarcity, heterogeneous frequency and spacing of sampling, and averaging or analysis procedures). Thus the coral-based estimate can provide an independent assessment of the robustness of historical climate variability. Conversely, we can use historical SST analyses to verify that the coral data faithfully record SST variability on the timescales of interest. In any case, if both the instrumental and coral data describe climatic phenomena, they should agree. Such intercomparison efforts are essential for the study of preinstrumental climate dynamics, and they provide an important link between paleoclimatological reconstruction efforts and the study of climate dynamics [*Fritts*, 1991; *Jones et al.*, 1996].

Here we argue that the coral δ^{18}O data may be used to resolve large-scale patterns of SST variability. While the hypothesis is not new, its testing using all available long δ^{18}O records simultaneously has not yet been attempted, mainly because of severe spatial and temporal gaps in the data sets of observed SST and coral δ^{18}O. The novelty of this work, which allows us to identify large-scale patterns of SST-δ^{18}O covariability, is in the systematic use of optimal interpolation to fill gaps in both data sets. Neither of the resulting analyses are problem-free, but in keeping with the hypothesis posed above, we presume climatic significance of their covariability. In section 2 we briefly describe the intercomparison data sets, and in section 3 we outline our approach and assumptions. Section 4 presents results of local and global intercomparisons of coral δ^{18}O and historical SST. We next explore the extent to which large-scale patterns of SST variability may be recovered from the sparse observational network of coral δ^{18}O data in section 5, and conclude by discussing the potential for reconstruction of large-scale patterns of SST variability using the results presented here. This understanding will be crucial for our ultimate goal, to be presented in a future paper: the systematic, objective reconstruction of SST and other climatically important fields from proxy data for the period prior to the rise of widespread instrumental observations.

2. Intercomparison Data

2.1. Sea Surface Temperature Data

Our source of SST anomaly data is the recently produced analysis [*Kaplan et al.*, 1998] of the MOHSST5 [*Parker et al.*, 1994] product of the U.K. Meteorological Office. MOHSST5 is a $5^o \times 5^o$ monthly compilation of historical (1856-1991) ship-based observations of SST, quality-controlled for obvious outliers and corrected for estimated observational biases. The analysis of this observational data set employs the newly developed technique of the reduced space optimal smoother to objectively extract large-scale variations of SST on a near-global grid (40^{o}S-60^{o}N) from incomplete spatial and temporal observations. The small-scale features of SST variability, amounting to $(0.3\text{-}0.4)^2(^o\text{C})^2$ of the local intermonthly variance but which are not constrained by the observed data, are filtered out in this approach. *Kaplan et al.* [1997, 1998] discuss the approach in detail, providing error estimates, numerous verification exercises and tests of the robustness, strengths, and limitations of the analyzed fields. For our purposes we will use annual (April to March) means for the period 1856-1990 from this SST analysis for comparisons with like averages of the coral data, as this definition is more appropriate than January to December for the tropics [*Ropelewski and Halpert*, 1987]. We assume that this SST analysis product sufficiently resolves the large-scale patterns of SST variability that we seek to represent in the coral data. However, no existing historical analysis of global SST fields is free of problems because of severe data deficiencies [*Hurrell and Trenberth*, 1999]. Specific problems and prospects of the analysis techniques used here are discussed by *Kaplan et al.* [1999].

2.2. Coral δ^{18}O Data

Beginning with the work of *Weber and Woodhead* [1972] and with roots in the work of *Epstein et al.* [1953], many studies have shown that the oxygen isotopic composition of coralline aragonite ($\delta^{18}O_{\text{coral}}$) is a function of both the SST in which the coral precipitated its skeletal material [*Fairbanks and Dodge*, 1979; *McConnaughey*, 1989; *Aharon*, 1991; *Shen et al.*, 1992; *Wellington et al.*, 1996] and seawater δ^{18}O ($\delta^{18}O_{\text{sw}}$) variability; the latter, in turn, depends on the local net runoff-evaporation--precipitation balance [*Cole and Fairbanks*, 1990; *Cole et al.*, 1993; *McCulloch et al.*, 1994; *Gat*, 1996; *Fairbanks et al.*, 1997]. In addition, the mean δ^{18}O of coralline aragonite is offset from sea water, most likely by biological processes [*McConnaughey*, 1989]. If this disequilibrium is assumed constant in time, then the functional relationship between $\delta^{18}O_{\text{coral}}$, SST, and $\delta^{18}O_{\text{sw}}$ may be linearized as

$$\delta^{18}O_{\text{coral}} = h\text{SST} + b\delta^{18}O_{\text{sw}} + \text{constant} + \text{error} \quad (1)$$

where h and b are empirically determined coefficients consistent with theoretical considerations [*McCrea*, 1950; *Epstein et al.*, 1953; *Dansgaard*, 1964]. Here we use all 12 long ($\geq$50 year) coral δ^{18}O records available from the World Data Center-A for Paleoclimatology

Table 1. Coral δ^{18}O Records Employed in This Work

Site	Name	Location	Time Period	Genus	Reference
Aqaba	AQ18	29.5°N, 35°E	1788-1992:A	*Porites*	*Heiss* [1994]
Aqaba	AQ19	29.5°N, 35°E	1886-1992:A	*Porites*	*Heiss* [1994]
Cebu	CEB	10°N, 124°E	1859-1979:A	*Porites*	*Patzöld* [1984]
Secas Island	SEC	8.0°N, 82.0°W	1708-1984:M	*Porites*	*Linsley et al.* [1994]
Kiritimati	KIR	2°N, 157°W	1938-1993:M	*Porites*	*Evans et al.* [1999]
Tarawa Atoll	TAR	1°N, 172°E	1894-1989:M	*Porites*	*Cole et al.* [1993]
Urvina Bay	URV	0.4°S, 91.2°W	1607-1953,62-81:A	*Pavona*	*Dunbar et al.* [1994]
Punta Pitt	PUN	0.7°S, 89°W	1936-1983:S	*Pavona*	*Shen et al.* [1992]
Mahe, Seychelles	MAH	4.6°S, 55.8°E	1846-1995:M	*Porites*	*Charles et al.* [1997]
Madang, PNG	MAD	5.2°S, 145.9°E	1922-1991:S	*Porites*	*Tudhope et al.* [1995]
Espiritu Santo	ESP	15°S, 167°E	1806-1979:A	*Platygyra*	*Quinn et al.* [1993]
New Caledonia	CAL	20.7°S, 166.2°E	1660-1991:S	*Porites*	*Quinn et al.* [1998]
Abraham Reef	ABR	22°S, 153°E	1635-1957:B	*Porites*	*Druffel and Griffin* [1993]

Nominal temporal resolution of δ^{18}O data: M, monthly; S, seasonal; A, annual; B, biennial. Sites are ordered in decreasing latitude (north to south).

(ftp.ngdc.noaa.gov/paleo/coral/) and the δ^{18}O record of *Patzöld* [1984] for intercomparison with SST. These records are listed in Table 1 in order of their length, and their locations are shown in Figure 1. Resolution of the records vary from monthly (TAR, KIR, MAH, and SEC) to seasonal (MAD, CAL, and PUN) to annual (AQ18, AQ19, CEB, URV, and ESP) to biennial (ABR). We calculate anomalies relative to the seasonal cycle (if any is resolved in the data) and form annual (April-March mean) averages for comparison with SST. However, we make no attempt to prescreen these data, as characterization of the data in terms of its ability to reliably contribute to the estimation of SST is one goal of this study. However, two caveats may be mentioned: (1) the Aqaba 19 record is from a core drilled horizontally, a practice avoided by many researchers seeking to minimize growth-related effects upon derived climate records [*de Villiers et al.*, 1995; G. Heiss, personal communication, 1998; J. Cole, personal communication, 1998]; (2) corals with subannual sampling resolution are likely to have smaller age model errors and better defined annually averaged δ^{18}O anomalies. While there is not enough data to perform systematic comparisons of these effects, the latter problem has been addressed in other studies [*Quinn et al.*, 1996, 1998].

3. Approach and Assumptions

3.1. Local Regression of δ^{18}O Anomaly on SST Anomaly

We begin our intercomparison by forming the regression of the δ^{18}O anomaly data on like averages of the *Kaplan et al.* [1998] SST anomaly estimates interpolated to the coral location. Thus we test the linear model

$$\delta^{18}\text{O anomaly} = h\text{SST anomaly} + \epsilon, \qquad (2)$$

where h is constant, seawater δ^{18}O is assumed insignificant insofar as it does not covary with local SST anomaly, and ϵ is the error in the relationship. By working in terms of SST and δ^{18}O anomalies relative to the mean seasonal cycle we eliminate from equation (2) the constant which is responsible for much of the error in equation (1) [*Crowley et al.*, 1999; *Guilderson*, 1997]. Once we have found the best fit h, we can evaluate the mean observational error ($\sqrt{\langle\epsilon^2\rangle}$) by calculating the residual

$$\epsilon = \sqrt{\langle(\delta^{18}\text{O} - h\text{SST})^2\rangle} \qquad (3)$$

where angle brackets indicate time averaging and δ^{18}O and SST are anomalies. As formulated, ϵ includes the error in SST observation by means of δ^{18}O due to proxy measurement and age model uncertainty, as well as error due to our sea water and equilibrium δ^{18}O assumptions. Hereafter we call it the "observational error" [*Evans et al.*, 1999]. Use of equation (2) has two advantages over previous calibration exercises: (1) by comparing mean annual averages to gridded SST anomaly estimates we obtain h for interannual and lower-frequency variability on 5°×5° or greater spatial scales, which is the signal of interest here; (2) with up to 135 independent observations for each regression estimate, significance tests for regressions and correlations are feasible. To test the ability of the coral δ^{18}O data to capture local low-frequency SST variability, we report the correlations between 5 and 11 year running boxcar means of the δ^{18}O and SST anomaly data. To establish whether the coral data may also capture nonlocal SST variability associated with ENSO, we calculate the correlation

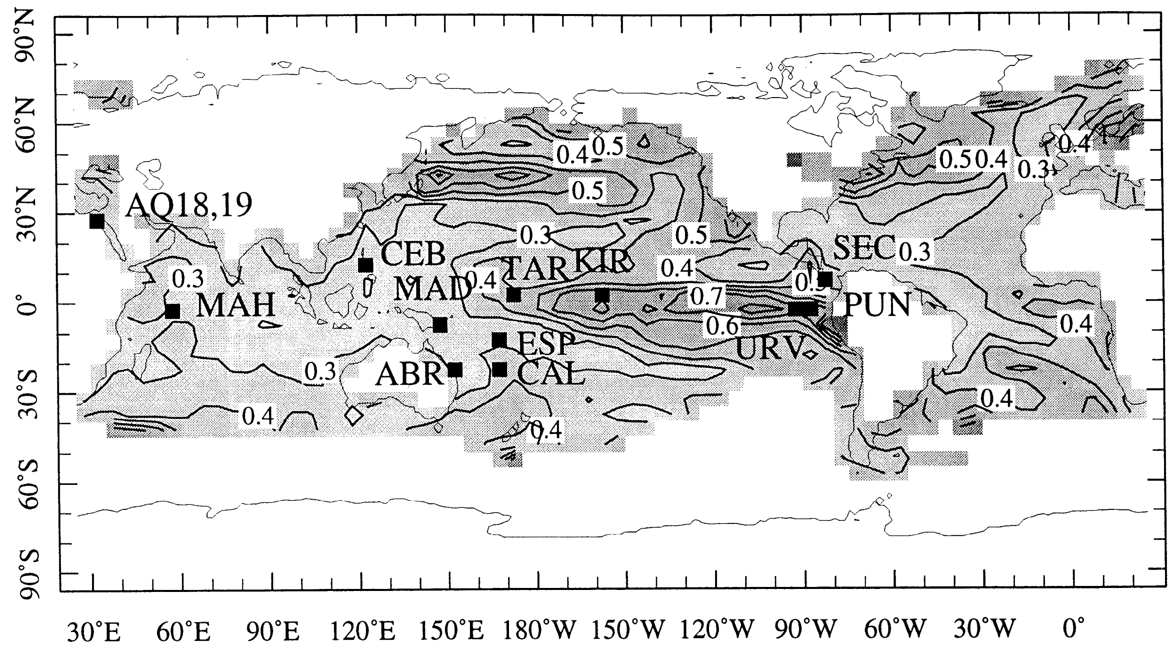

Figure 1. Sampling sites for the 13 coral data sets examined in this study. Contours give the RMS SST anomaly from the *Kaplan et al.* [1998] analysis (contour interval: 0.1°C). Site names are abbreviated as in Table 1.

between the 1, 5, and 11 year averages of δ^{18}O data and NINO3 SST anomaly index (SST anomaly averaged over the region (5°N-5°S, 150°W - 90°W)).

3.2. EOF Analysis of the Coral Data

We expect that signals evident across the areally extensive network of coral sites are of large scale and climatically interpretable. In turn we hypothesize that nonclimatic influences are site-specific and therefore uncorrelated between the individual coral time series. We test this hypothesis by performing empirical orthogonal function (EOF) analysis of the standardized coral δ^{18}O data and analyzing the leading patterns of common variability that emerge, in the sense of *Bretherton et al.* [1992]. There is no single established procedure for these kinds of analyses when there are missing data in the samples. We first analyze the set of coral δ^{18}O records by performing an optimal interpolation (OI) [*Daley*, 1991] on it, using the location×location covariance matrix estimated from all coral δ^{18}O data available for the comparison period (1856–1990). With the exception of the covariances of Abraham Reef with Kiritimati, Punta Pitt, and Madang, each element in the covariance matrix is estimated using at least 33 common observations. The eigenvalues of the covariance matrix are all positive, indicating that the covariance matrix is positive definite and invertible, and no truncation is necessary to achieve a stable solution. In the analysis procedure we conservatively assume all measurements are made with an identical observational error r = 0.5 standard deviation units (equation 3). This choice of r guarantees that when coral data are available, the OI solution will be highly correlated with the original records (correlation($\delta^{18}O_{obs}$, $\delta^{18}O_{OI}$) $\geq$0.9). For years when there are no coral data available at a given site the OI emphasizes common cross-site features which are observed in the covariance estimate; thus this analysis is consistent with our general purpose of using the coral data to represent broad-scale features of SST variability.

To assess the quality of the SST information extracted from the OI-analyzed δ^{18}O data, we also perform a parallel EOF analysis separately on normalized SST anomaly data from the coral sampling sites; the SST data are from *Kaplan et al.* [1998]. We compare the results of the coral EOF analysis to this benchmark experiment.

3.3. SVD Analysis of Coral δ^{18}O and Historical SST Anomaly

If the leading patterns of variability in both the coral data and the SST observations are describing the same phenomena, then they should agree (section 1). To test this hypothesis, we also performed two separate singular value decomposition (SVD) analyses: (1) analysis of the covariance between the 13 OI-interpolated coral records and the leading 80 principal components of the EOFs of SST anomaly covariance, as estimated by *Kaplan et al.*

Table 2. Regression Statistics for Coral δ^{18}O Data, 1856–1990

Name	Number of Years N	std(δ^{18}O), ‰, PDB	std(SST), °C	Correlation,[a] unitless	Regression, ‰/°C	Error, ‰	Signal/Noise, unitless
AQ18	135	0.13	0.31	-0.25(78)[b]	-0.10(78)[b]	0.13	1.03
AQ19	106	0.16	0.31	-0.28(29)	-0.15(29)	0.15	1.04
CEB	115	0.22	0.18	-0.22(84)[b]	-0.27(84)[b]	0.22	1.03
SEC	128	0.16	0.34	-0.20(97)[b]	-0.10(97)[b]	0.16	1.02
KIR	53	0.19	0.72	-0.72(21)[c]	-0.19(21)[c]	0.13	1.43
TAR	95	0.16	0.45	-0.56(37)[c]	-0.21(37)[c]	0.14	1.21
URV	113	0.19	0.63	-0.37(111)[c]	-0.11(111)[c]	0.17	1.07
PUN	45	0.15	0.64	-0.76(43)[c]	-0.18(43)[c]	0.10	1.53
MAH	135	0.10	0.27	-0.57(27)[c]	-0.20(27)[c]	0.08	1.21
MAD	68	0.16	0.24	-0.51(36)[c]	-0.34(36)[c]	0.14	1.16
ESP	124	0.18	0.28	-0.08(62)	-0.05(62)	0.18	1.00
CAL	135	0.17	0.30	-0.49(19)[b]	-0.28(19)[b]	0.15	1.15
ABR	56	0.19	0.20	0.06(54)	0.06(54)	0.19	1.00

Here std is standard deviation, and PDB is the reference standard Pee Dee Belemnite.
[a]Significance of regressions and correlations determined using Student's t test [*Sokal and Rohlf*, 1995]; estimated effective number of degrees of freedom [*Trenberth*, 1984] are in parentheses.
[b]Significance is at 95% confidence level.
[c]Significance is at 99% confidence level.

[1998] and (2) analysis of the covariance between the normalized SST time series from the 13 coral locations and the analyzed fields of SST anomaly from *Kaplan et al.* [1998]. The SVD procedure applied to cross-covariance matrices finds pairs of spatial patterns which maximize the explained covariance between the two fields [*Bretherton et al.*, 1992]. The SVD analyses essentially filter the information retrieved from the sparse observational network (comprised of either coral δ^{18}O or SST at the coral locations) for patterns of variability shared with the SST field. As with the EOF analysis, the purpose of making these parallel SVD analyses was to compare the patterns recoverable from the sparse coral sampling network to the results obtained from a benchmark consisting of a similarly sparse network of SST data. We used the results of the SVD analyses to construct the leading modes recoverable from the δ^{18}O data and from the sparse SST data network.

4. SST-Coral δ^{18}O Intercomparison

4.1. Regression of δ^{18}O on Local SST Anomaly

Table 2 gives statistics for regression of coral δ^{18}O anomaly on analyzed SST anomaly given the linear model: $\delta^{18}\text{O} = h\text{SST anomaly} + \epsilon$. With the exception of h calculated for Abraham Reef and Espiritu Santo (neither of which have statistically significant correlation or regression on local SST at the 90% confidence level), the regression coefficients range from -0.10 to -0.34‰/°C. For values significantly different from zero at or above the 95% confidence level (10 corals) the mean regression slope is -0.20‰/°C, with mean RMS error in predicted δ^{18}O of 0.14‰ (Table 2). The mean regression and RMS errors for significant *Porites* genus corals (Aqaba 19, Cebu, Tarawa, Kiritimati, New Caledonia, Secas, Madang and Mahe) are -0.19‰/°C and 0.15‰, respectively.

The mean regressions calculated for these subsets of the data are equivalent to the regression found by *Weber and Woodhead* [1972], when their coral δ^{18}O data is corrected for differences in mean annual seawater δ^{18}O between locations sampled in their study [*Guilderson*, 1997]. Our result is also consistent with many previous calibration studies comparing local SST observations to coral δ^{18}O data for individual sites, at monthly to annual temporal resolution, for a variety of coral genera. These studies report regression slopes in the range -0.18 to -0.22‰/°C [*Fairbanks and Dodge*, 1979; *Patzöld*, 1984; *McConnaughey*, 1989; *Shen et al.*, 1992; *Dunbar et al.*, 1994; *Wellington et al.*, 1996; *Guilderson*, 1997; *Quinn et al.*, 1998; *Evans et al.*, 1998a]. The results suggest that coral δ^{18}O anomaly may be predicted from annually averaged, local (i.e., 5°×5°) SST anomaly with observational error of ≈ 0.14‰, and signal:error ratio of 1-1.5. This error is equivalent to ≈ 0.4°-1.2°C RMS. Further, since the local regressions we calculate are similar to those of *Weber and Woodhead* [1972] as analyzed by *Guilderson* [1997], the results also suggest that on annual timescales the error introduced by local seawater δ^{18}O variability independent of local SST variability is minimal. Much of the regression uncertainty may instead be due to limited SST-δ^{18}O calibration ranges.

Table 3. Comparison of Coral δ^{18}O Data with Local and Large-Scale SST Variability, 1856-1990

Name	Correlations[a]		Correlations[a] After Averaging				Correlations[a] With SVD Time Series		
	SST_{loc}	NINO3	5 year SST_{loc}	5 year NINO3	11 year SST_{loc}	11 year NINO3	First (ENSO)	Second (Trend)	Third (PDO)
AQ18	-0.25(78)[b]	-0.01(78)	-0.61(25)[c]	-0.02(25)	-0.72(10)[c]	0.09(10)	0.11(78)	-0.29(16)	0.73(48)[c]
AQ19	-0.28(29)	0.00(29)	-0.19(19)	0.16(19)	-0.17(8)	0.24(8)	0.27(29)	-0.60(16)[c]	-0.00(29)
CEB	-0.22(84)[b]	0.06(84)	-0.18(21)	0.17(21)	-0.23(9)	0.25(9)	0.13(79)	-0.55(16)[c]	-0.15(48)
SEC	-0.20(97)[b]	-0.12(97)	-0.41(24)[b]	-0.07(24)	-0.50(10)[d]	0.18(10)	0.14(79)	-0.33(16)	-0.40(48)[c]
KIR	-0.72(21)[c]	-0.79(21)[c]	-0.33(9)	-0.72(9)[b]	-0.04(5)	-0.70(5)[d]	0.88(21)[c]	0.63(16)[c]	0.06(21)
TAR	-0.56(37)[c]	-0.71(37)[c]	-0.44(17)[b]	-0.58(17)[c]	-0.52(7)	-0.59(7)[d]	0.77(37)[c]	0.23(16)	-0.14(37)
URV	-0.37(111)[c]	-0.36(111)[c]	-0.28(21)	-0.17(21)	-0.37(8)	-0.10(8)	0.63(79)[c]	0.47(16)[b]	-0.27(48)[b]
PUN	-0.76(43)[c]	-0.74(43)[c]	-0.56(7)[d]	-0.68(7)[b]	-0.53(4)	-0.67(4)	0.85(43)[c]	0.56(16)[c]	-0.30(43)[c]
MAH	-0.57(27)[c]	-0.34(27)[d]	-0.51(25)[c]	-0.11(25)	-0.59(10)[b]	0.12(10)	0.51(27)[c]	-0.56(16)[c]	0.12(27)
MAD	-0.51(36)[c]	0.49(36)[b]	-0.51(12)[b]	0.26(12)	-0.70(4)[d]	0.24(4)	-0.44(36)[c]	-0.63(16)[c]	-0.02(36)
ESP	-0.08(62)	0.28(62)[b]	0.18(23)	0.22(23)	0.41(9)	-0.08(9)	-0.53(62)[c]	0.27(16)	0.40(48)[c]
CAL	-0.49(19)[b]	0.16(19)	-0.72(19)[c]	0.21(19)	-0.77(10)[c]	0.32(10)	-0.14(19)	-0.77(16)[c]	-0.24(19)
ABR	0.06(54)	0.10(54)	0.32(9)	0.13(9)	0.36(3)	-0.10(3)	-0.28(54)[b]	-0.07(16)	0.14(48)

[a]Significance of correlations determined using Student's t-test [*Sokal and Rohlf*, 1995]; estimated effective number of degrees of freedom [*Trenberth*, 1984] are in parentheses.
[b]Significance is at the 95% level.
[c]Significance is at the 99% level.
[d]Significance is at the 90% level.

4.2. Correlation of δ^{18}O With Local and Large-Scale SST Anomaly

Table 3 shows that corals in ENSO-affected regions, primarily in the equatorial oceans (Figure 1), provide the best correlations with local SST anomaly: Tarawa, Kiritimati, Urvina Bay, Punta Pitt, Madang, and Mahe δ^{18}O-SST correlations are significant at the 99% level. However, many of these and other δ^{18}O time series have significant correlation with SST in remote regions as well. These patterns can have real physical bases, which may be underlain by either the spatial covariance of SST (see equation (4) and discussion below) or the covariance of SST with seawater δ^{18}O variability (see equation (1)).

Two representative examples are shown in Figure 2. Figures 2a and 2b show the correlations of the Kiritimati and Tarawa δ^{18}O time series with the global SST anomaly field, respectively. At the grid point closest to the location of the coral sampling sites, the corresponding regressions equal those reported in Table 2. This local regression is then used to predict coral δ^{18}O, and the residual of the regression is the difference between the δ^{18}O time series and the prediction. The correlation of the local regression residual with the global SST field is plotted in Figures 2c and 2d, respectively. This second row in Figure 2 is intended to illustrate the extent to which the pattern correlations shown in the top row of Figure 2 are not explained by SST field covariance witl local SST. As we expect the residual δ^{18}O time serie to reflect net freshwater flux anomalies (equation (1)) Figures 2c and 2d should show the extent to which the patterns in Figures 2a and 2b are determined by globa SST covariance with local seawater δ^{18}O anomaly.

For example, the Kiritimati δ^{18}O record (Figure 2a is highly correlated with local SST, which is in turn correlated with the basin-wide pattern of SST variabilit associated with ENSO [*Evans et al.*, 1999]. Little significant correlation is obtained from the residual of the regression on local SST (Figure 2b); the ENSO pattern i retrieved through covariance with Kiritimati-local SST which is, in turn, mimicked by the KIR δ^{18}O record A similar ENSO pattern is mainly retrieved througl correlation of the SST field with the residual to the regression of Tarawa δ^{18}O on Tarawa local SST (Figur 2d). This has been documented by *Cole et al.* [199 and reflects seawater δ^{18}O anomalies at Tarawa during ENSO events. Net precipitation lowers the δ^{18}O content of seawater by mixing in isotopically deplete rainwater [*Gat*, 1996; *Fairbanks et al.*, 1997], an effec which is proportional to the observed change in cora δ^{18}O and is negatively correlated with local SST [*Webe and Woodhead*, 1972; *Fairbanks et al.*, 1997], equatio (1). This makes the Tarawa record better correlate with NINO3 SST anomaly than with local temperatur because anomalously heavy rainfall in the central and eastern equatorial Pacific is part of ENSO dynamics and is positively correlated with NINO3. In fact, ENSO covariant changes in seawater δ^{18}O [*Cole et al.*, 1993; *Dunbar et al.*, 1994; *Wellington et al.*, 1996; *Evans et al.*, 1999] make the Kiritimati, Punta Pitt, and Urvina Bay records as good or better ENSO recorders than if they simply monitored local SST variability alone. We interpret these results to suggest that the coral δ^{18}O may also provide significant information on basin-scale SST variability associated with ENSO.

Our analysis of the SST field variability associated with the δ^{18}O data suggests that we modify equation (2) to extract the most climatic information possible from each coral record by using a nonlocal model of δ^{18}O-SST anomaly dependence:

$$\delta^{18}O = \mathbf{HT} + \epsilon \qquad (4)$$

where δ^{18}O is now the set of all coral δ^{18}O time series, **H** is now a set of patterns which may have basin-wide or even global spatial scale, and **T** is the spatiotemporal SST anomaly field. Note that while we expect **H** to approach h in value locally, it need not be so globally.

However, at least some of the lower-frequency or secular features in the δ^{18}O records may originate in influences on the δ^{18}O of coral aragonite (equation (1)) which do not covary with the SST field or seawater δ^{18}O variability. With the exception of AQ18 and CAL, temporal smoothing does not improve correlation with local SST anomaly (Table 3). Temporal smoothing should eliminate possible age model errors as the reason for low annual correlations, as all of age models considered here have estimated uncertainties of less than ± 5 years. Nevertheless, even the high annual correlations for subannually sampled equatorial sites decrease considerably for 5 or 11 year running means and lose their statistical significance; while correlations for some off-equatorial sites (CEB, ABR, and ESP) improve, they do not reach statistical significance. Yet on interannual and decadal timescales the influence of very local climate effects (e.g., the difference between pointwise SST values and averages for $5^o \times 5^o$ boxes which we use for intercomparison) is unlikely to be significant.

We are left with the speculation that some of the low-frequency variability evident in the δ^{18}O time series extracted from individual corals may be a func-

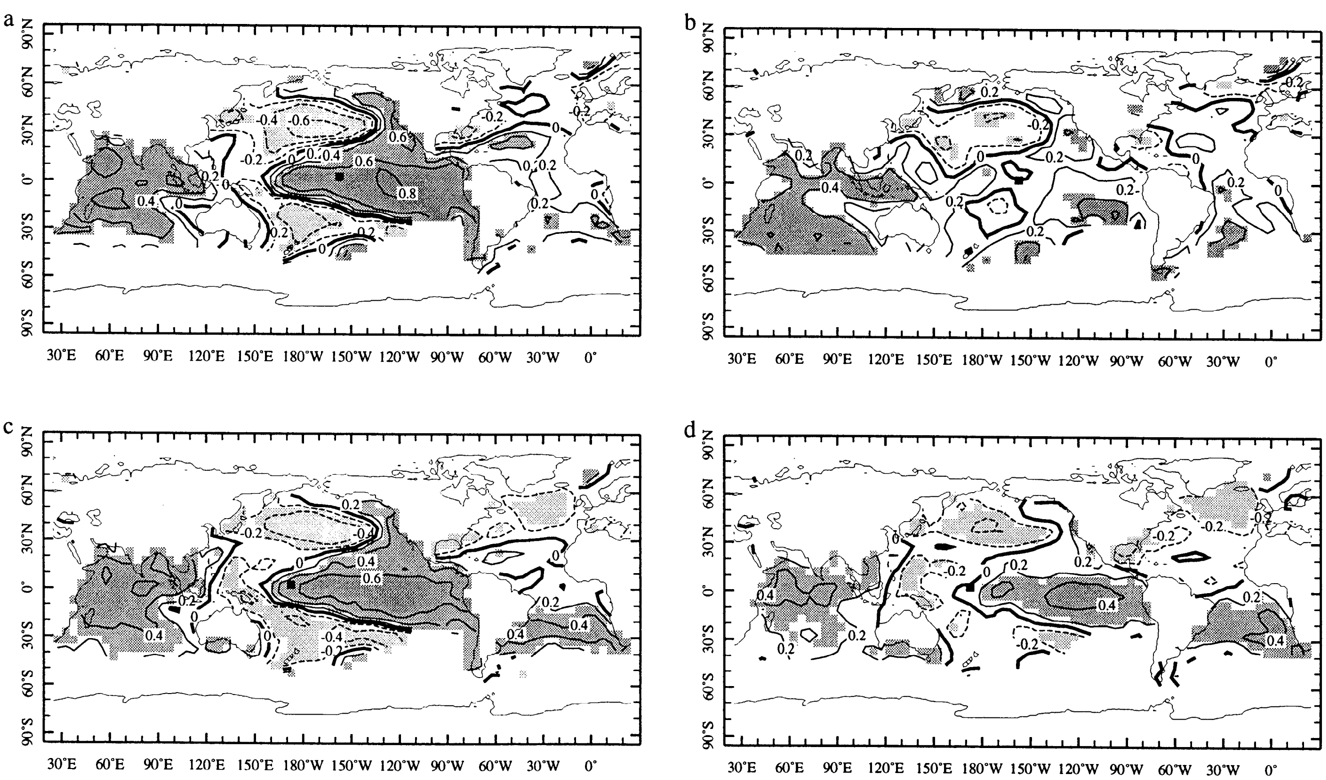

Figure 2. The SST pattern associated with the El Niño-Southern Oscillation (ENSO) characterized in two coral δ^{18}O records. Correlation of the SST field of *Kaplan et al.* [1998] with (a) KIR, annual averages, 1938–1990; (b) residual of the regression of KIR on local SST, annual averages, 1938–1990 (c) TAR, annual averages, 1895–1989; and (d) residual of the regression of TAR on local SST, annual averages, 1895–1989. Shaded areas show correlations significant at or above the 90% confidence level [*Trenberth*, 1984]. Solid squares show coral sampling sites.

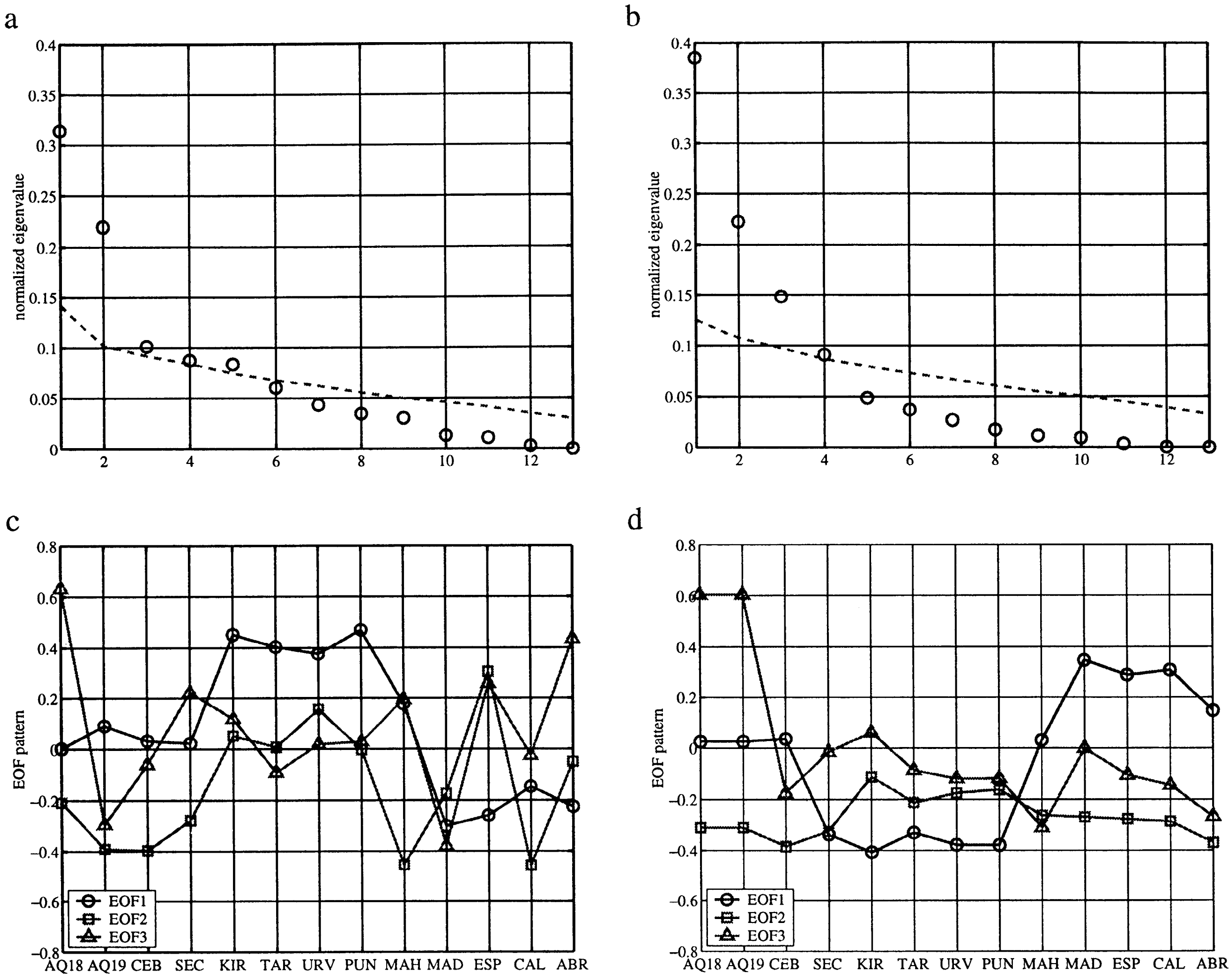

Figure 3. EOF analysis of the coral $\delta^{18}O$ data and of the SST data from the coral sampling locations. (a) Eigenvalue trace normalized to the sum of the variance in the data set. The 95% confidence interval based on 100 random time series with autoregressive characteristics of the coral data is shown as a dashed line [*Preisendorfer*, 1988]. (b) As in Figure 3a, except for SST data from the coral locations. (c) First three EOF patterns as a function of coral site. (d) As in Figure 3c, except for SST data from the coral locations. Site abbreviations are as in Table 1. Sites are ordered by descending latitude (north to south).

tion of variability in the mean disequilibrium between coral $\delta^{18}O$ and seawater $\delta^{18}O$ which may have a complex biological or ecological origin. These effects, which we term nonclimatic, may dominate when strong interannual ENSO variability is filtered out by smoothing and can mask an underlying lower-frequency, smaller-amplitude climatic signal in either SST or SST covariant changes in seawater $\delta^{18}O$. Indeed, many workers have reported long-term trends in coral $\delta^{18}O$ data that are consistent in sign but are too large to be explained by observed changes in SST, seawater salinity, or rainfall over contemporaneous intervals [*Cole et al.*, 1993; *Druffel and Griffin*, 1993; *Dunbar et al.*, 1994; *Heiss*, 1994; *Quinn et al.*, 1996; *Charles et al.*, 1997; *Quinn et al.*, 1998; *Evans et al.*, 1999; A. Cohen, personal communication, 1999]. Similar considerations may explain some of the differences between the subannual and annual SST-$\delta^{18}O$ calibrations reported by *Crowley et al* [1999].

5. Identification of the Large-Scale SST Signal in the Coral Data

Intercomparison results thus far suggest that indi vidual coral records are best for SST extraction in th limited ENSO frequency interval, provided the prope location is sampled. A complimentary result was sug gested in a derivation of a hypothetical "optimal" cora sampling site network [*Evans et al.*, 1998b]. Howeve the real coral network appears to contain significan large-scale, sometimes nonlocal SST information. I this case, patterns which explain variance across cora sites may better represent the climate information content of the corals than do the individual time series themselves.

Figure 3 shows the results of separate EOF analyses of the $\delta^{18}O$ and SST anomaly data from the coral locations. We find that the $\delta^{18}O$ data produce two EOFs with eigenvalues that are significant by Preisendorfer's Rule N [*Preisendorfer*, 1988] modified to take into account autocorrelation of data series; a third is almost significant (Figure 3a, dashed line). These three EOFs explain 77% of the variance in the coral data. By the same measure, EOF analysis of the SST data from the coral locations produces three significant EOFs (Figure 3b) and explains 63% of the variance. Correlations between the corresponding three $\delta^{18}O$ and SST principal components (PCs) are 0.69, -0.55, and -0.19, respectively. The first two of these correlations are significant at the 90% level, assuming 79 and 16 effective degrees of freedom in the cross-correlation estimates, respectively [*Trenberth*, 1984]. In both analyses the first EOF has high loadings at the ENSO-sensitive equatorial Pacific sites (Figures 3c and 3d); the second and third patterns, whose PCs contain trend and decadal temporal variability, are associated with the off-equatorial sites.

We diagnose these patterns further by correlating the leading three PCs corresponding to the first three $\delta^{18}O$ EOFs with indices of dominant large-scale climatic phenomena. The first is the time series of the SST anomaly pattern associated with ENSO; correlation of PC1 with NINO3 SST anomaly is -0.69. The second resembles a global warming-like pattern with eastern equatorial Pacific cooling, similar to that observed by *Cane et al.* [1997]; correlation of decadal averages with time is 0.81. The third pattern is poorly defined by both the $\delta^{18}O$ data and the SST anomaly data, which suggests that a third pattern is difficult to constrain with only 13 sampling locations. We speculate that it weakly resembles the spatial structure of the ENSO-like decadal variability observed in SST and sea level pressure data by *Zhang et al.* [1997] and in tree ring chronologies by *Villalba et al.* [1999] and *Evans et al.* [2000]. However, decadal correlation with sea level pressure anomaly averaged over the region (150°E-120°W, 30°N- 50°N) is only 0.27, not statistically significant. Together, the local regression and EOF analyses suggest that the climate signals may be masked by variability in individual $\delta^{18}O$ time series that is unrelated to large-scale SST variability. However, this variability appears local in nature and uncorrelated across sites. By seeking to explain the most variance across sites the leading EOFs filter out some of this "noise" and extract patterns from the $\delta^{18}O$ data which are climatically interpretable.

The climatic significance of the principal patterns found in the coral $\delta^{18}O$ data and in the SST data from the coral sites is further illustrated by SVD analysis with the complete historical SST field [*Kaplan et al.*, 1998]. The SVD analysis between coral records and SST fields retrieved the same characteristic patterns of SST variability as did the EOF analysis. However, the SVD analysis suggests that not only do the identified modes describe the leading patterns of cross-site $\delta^{18}O$ variability but also that these leading modes describe large-scale patterns of SST variability. The time series associated with the first three SVD modes are shown in Figure 4. The correlations of these time series with global SST anomaly are shown in Figure 5 and illustrate the spatial patterns associated with the SVD modes.

The contributions of individual coral time series toward the first three SVD modes are also interpretable and are illustrated as correlations with each coral $\delta^{18}O$ time series in the last three columns of Table 3. Coral sites located in ENSO-sensitive regions, such as the equatorial Pacific and Indian Oceans, best provide information on ENSO-related SST variability captured by SVD mode 1. Other sites, such as those in the off-equatorial locations, contribute more strongly to the decadal and secular modes of variability. Some records provided significant contributions to more than one of the SVD patterns. Certain sites seem to better capture SST variability associated with large-scale climatic patterns than others; while the locations of some of these sites are quite obvious (e.g., the central and eastern Pacific for monitoring ENSO variability), others are not so obvious (e.g., the western Pacific for trend pattern resolution and the northern Red Sea for perhaps tracking Atlantic and Pacific basin-centered decadal variability). As such, these results are broadly consistent with a more hypothetical approach to the observational array design problem solved in *Evans et al.* [1998b]. In particular, the sites identified there as most useful for reconstructing the NINO3 SST anomaly are similar to those identified here as most closely associated with SVD mode 1; those identified as the best sites for reconstruction of the global mean SST anomaly are similar in location to those associated with SVD mode 2.

In fact, ENSO and trend-sensitive corals (Table 3) show correlations with leading SVD modes that are as high or higher than their correlation with local SST. This suggests, as hypothesized in section 3.2, that the SVD analysis has successfully filtered out variance unrelated to large-scale SST variability. Although some of the $\delta^{18}O$ records contributing to the second and third SVD modes did not significantly correlate with local SST (e.g., AQ19, CEB, ESP, and ABR; Table 2), these SVD modes are also supported by several other $\delta^{18}O$ records that do (AQ18, SEC, MAH, MAD, URV, and CAL). Of the two Aqaba records, vertically drilled AQ18 correlated significantly with local SST and with SVD mode 3; horizontally drilled AQ19 correlated with

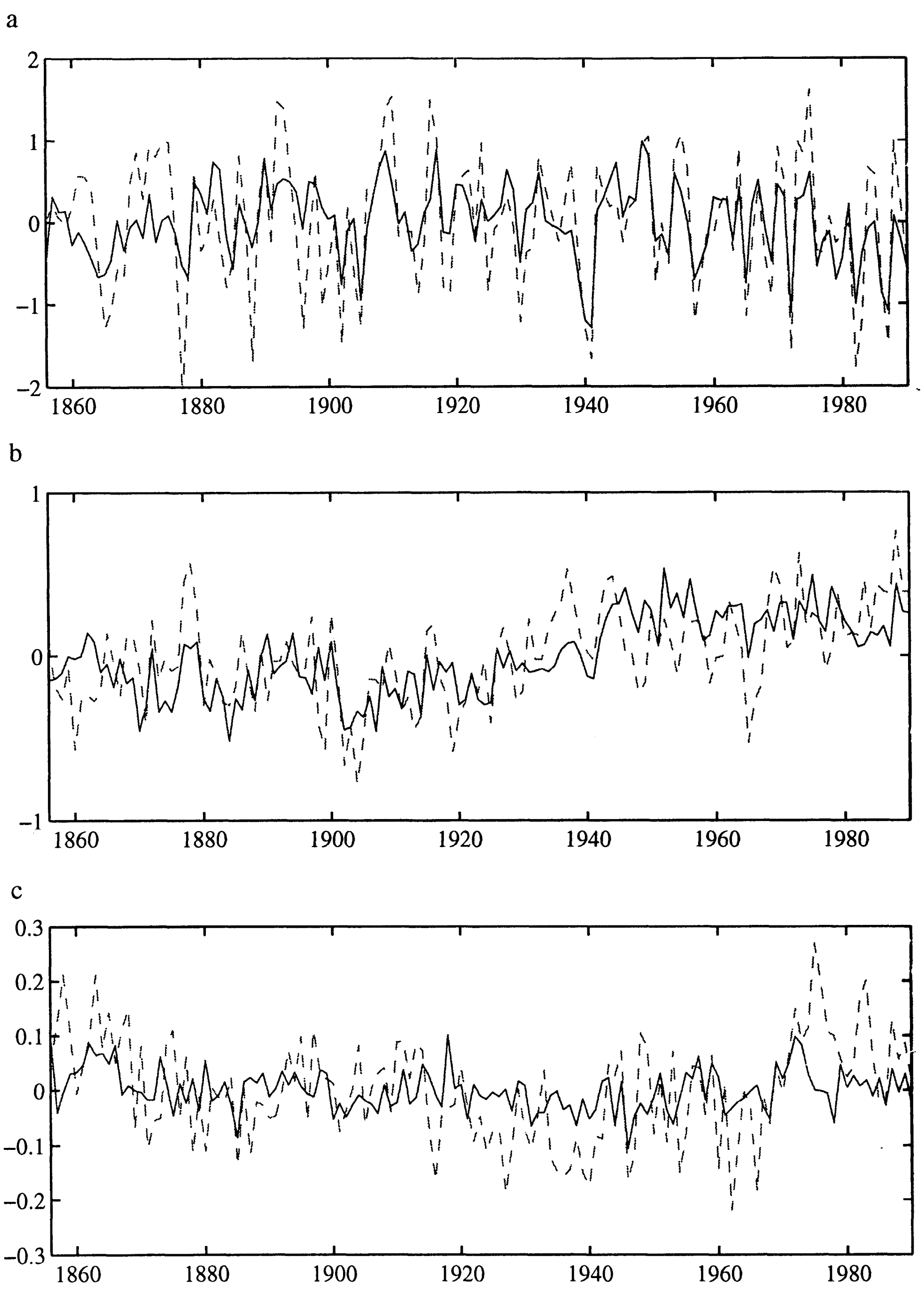

Figure 4. Singular value decomposition (SVD) analysis of the coral $\delta^{18}O$ and SST data at the coral locations. (a) Time series 1. (b) Time series 2. (c) Time series 3. Solid lines represent $\delta^{18}O$ data, and dashed lines represent SST data.

SVD mode 2 but not local SST. These results defy interpretation but may suggest that $\delta^{18}O$ data derived from the potentially suboptimal horizontal growth axes may be suitable for resolution of patterns associated with long timescales, such as a secular trend. Alternatively, it may be most prudent to consider information derived from horizontally oriented cores as suspect. Annually averaged $\delta^{18}O$ anomalies from Secas Island (SEC), known to be driven by local seawater $\delta^{18}O$ variability [*Linsley et al.*, 1994], show no correlation to SST anywhere other than locally. However, on pentadal an decadal timescales the record helps resolve the thir SVD pattern. Of all the corals examined only AB] did not show significant correlation with local SST c NINO3 on annual, pentadal, or decadal timescales, pe haps owing to its biennial sampling resolution (Table 1 Nevertheless, even this record shows significant correl tion with the first SVD time series (Table 3). Resan pling at a higher resolution may produce better resul from this site. Similarly, better age control and finer re olution sampling in the Punta Pitt (PUN) record may partially explain why PUN correlates more highly with the ENSO SVD mode than does the Urvina Bay (URV) data series.

These results suggest that even a sparse observational network may be useful for the reconstruction of large-scale SST patterns at times prior to the intercomparison period. On the other hand, we expect that the mere handful of coral $\delta^{18}O$ data examined here will resolve the large-scale SST patterns with quite large errors (equation (4)). The second and third patterns are not statistically significant in many places (Figure 5). The third pattern is resolved by perhaps only five contributors (AQ18, ESP, PUN, CAL, and SEC; Table 3). If these patterns are truly resolved by the coral data, then additional records from sites which resolve associated SST or seawater $\delta^{18}O$ variability should improve their definition and significance. Actual coral-based re-

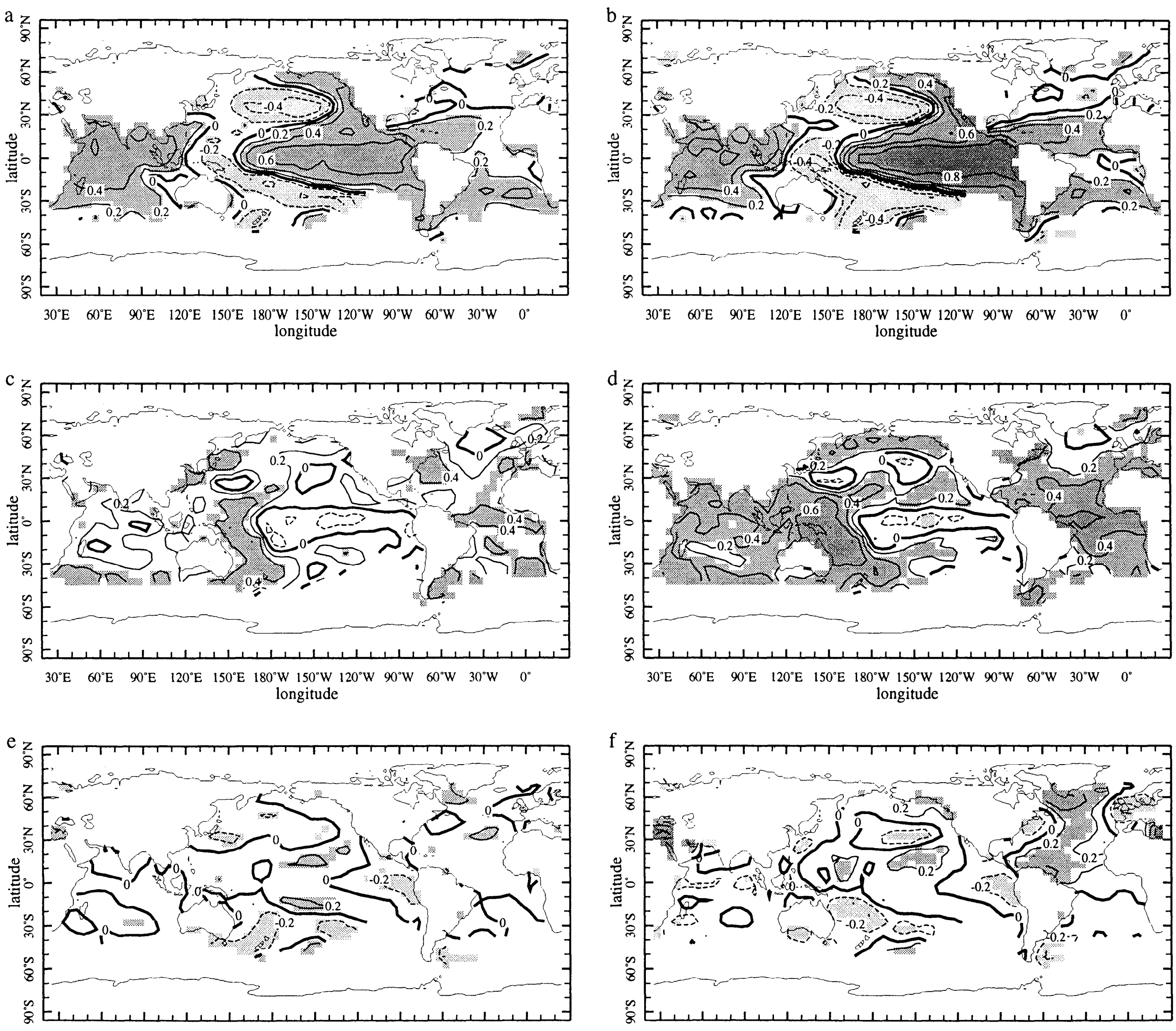

Figure 5. Contour plots of the correlation of the leading SVD modes with global SST anomaly. (a) Correlation of $\delta^{18}O$ SVD mode 1 with SST anomaly. (b) Correlation of SST SVD mode 1 with SST anomaly. (c) Correlation of $\delta^{18}O$ SVD mode 2 with SST anomaly. (d) Correlation of SST SVD mode 2 with SST anomaly. (e) Correlation of $\delta^{18}O$ SVD mode 3 with SST anomaly. (f) Correlation of SST SVD mode 3 with SST anomaly. Shading shows regions with correlations significant at or above the 90% confidence level [*Trenberth*, 1984].

construction of SST patterns will require careful verification via cross-validation experiments employing withheld historical SST observations.

6. Conclusion

We find that intercomparison of coral $\delta^{18}O$ data and historical analyzed SST data produces local regressions which are mainly consistent with the literature interpretation of coral $\delta^{18}O$ data as a proxy for local SST variability. However, additional climatic information is provided by these data on large spatial and long temporal scales. Despite the domination of individual coral $\delta^{18}O$ records by unknown but apparently localized influences on decadal and lower-frequency timescales, EOF analysis identifies three leading patterns of variability in the 13 coral data sets. These patterns are similar to those found by EOF analysis performed on SST data from the coral sites. They are climatically interpretable as the oceanographic signature of ENSO, a near-global warming trend in which the central and eastern equatorial Pacific cools, and a Pacific decadal ENSO-like pattern. These results suggest that SST field variability may be recoverable from even a sparse coral $\delta^{18}O$ observational network. They also demonstrate the potential for coral $\delta^{18}O$ time series to be used to reconstruct features of the SST anomaly field associated with these patterns well into the preinstrumental period. This potential should improve as additional coral data from critical regions become available and provide better resolution of the recoverable patterns.

Acknowledgments. This work was supported by NOAA/ESH grant NA86GP0437. D. Schrag suggested we validate the low-frequency signals evident in many coral records using local SST data. We thank D. Battisti and G. Shen for hosting a June 1997 JISAO workshop on intercomparison of instrumental and proxy data, at which we first presented the ideas developed here and received valuable feedback and encouragement from participants. We thank M. Eakin for encouragement and assistance with obtaining data sets. J. Cole and E. Druffel assisted with gathering coral data sets and gave advice concerning their use. J. Lough, G. Heiss, A. Tudhope, D. Hunter, and R. Dunbar made valuable comments on the analysis. T. Quinn shared the New Caledonia coral record and prepublication manuscripts. A. Giannini gave useful comments on an early manuscript. An anonymous review of another paper [*Evans et al.*, 1998b] elegantly made points similar to some of those raised here. We are grateful to three anonymous reviewers for their helpful comments. Not least, we thank the cited scientists who kindly made their published data available and the World Data Center-A for Paleoclimatology (http://www.ngdc.noaa.gov/paleo/paleo.html), which provided easy data access. LDEO contribution #6069.

References

Aharon, P., Recorders of reef environment histories: Stable isotopes in corals, giant clams, and calcareous algae, *Coral Reefs*, *10*, 71–90, 1991.

Bretherton, C. S., C. Smith, and J. M. Wallace, An intercomparison of methods for finding coupled patterns in climate data, *J. Clim.*, *5*, 541–560, 1992.

Cane, M. A., A. C. Clement, A. Kaplan, Y. Kushnir, R. Murtugudde, D. Pozdnyakov, R. Seager, and S. E. Zebiak, 20th century sea surface temperature trends, *Science*, *275*, 957–960, 1997.

Charles, C. D., D. E. Hunter, and R. G. Fairbanks, Interaction between the ENSO and the Asian monsoon in a coral record of tropical climate, *Science*, *277*, 925–928, 1997.

Cole, J. E., and R. G. Fairbanks, The Southern Oscillation recorded in the $\delta^{18}O$ of corals from Tarawa Atoll, *Paleoceanography*, *5*, 669–683, 1990.

Cole, J. E., R. G. Fairbanks, and G. T. Shen, Recent variability in the Southern Oscillation: Isotopic results from a Tarawa Atoll coral, *Science*, *260*, 1790–1793, 1993.

Crowley, T. J., T. M. Quinn, and W. T. Hyde, Validation of coral temperature calibrations, *Paleoceanography*, *14*, 605–615, 1999.

Daley, R., *Atmospheric Data Analysis*, *Atmos. Space Sci. Ser.*, vol. 2, Cambridge Univ. Press, New York, 1991.

Dansgaard, W., Stable isotopes in precipitation, *Tellus*, *16*, 436–468, 1964.

de Villiers, S., B. K. Nelson, and A. R. Chivas, Biological controls on coral Sr/Ca and $\delta^{18}O$ reconstructions of sea surface temperatures, *Science*, *269*, 1247–1249, 1995.

Druffel, E. R. M., and S. Griffin, Large variations of surface ocean radiocarbon: Evidence of circulation changes in the southwestern Pacific, *J. Geophys. Res.*, *98*, 20,246–20,259, 1993.

Dunbar, R. B., and J. E. Cole, *Coral Records of Ocean-Atmosphere Variability: Report From the Workshop on Coral Paleoclimate Reconstruction*, Natl. Oceanic and Atmos. Admin., Silver Spring, Md., 1993.

Dunbar, R. B., G. M. Wellington, M. W. Colgan, and P. W. Glynn, Eastern Pacific sea surface temperature since 1600 A.D.: The $\delta^{18}O$ record of climate variability in Galápagos corals, *Paleoceanography*, *9*, 291–315, 1994.

Epstein, S., R. Buchsbaum, H. A. Lowenstam, and H. C. Urey, Revised carbonate-water isotopic temperature scale, *Geol. Soc. Am. Bull.*, *64*, 1315–1326, 1953.

Evans, M. N., R. G. Fairbanks, and J. L. Rubenstone, A proxy index of climate teleconnections from the central equatorial Pacific, *Nature*, *394*, 732–733, 1998a.

Evans, M. N., A. Kaplan, and M. A. Cane, Optimal sites for coral-based reconstruction of sea surface temperature, *Paleoceanography*, *13*, 502–516, 1998b.

Evans, M. N., R. G. Fairbanks, and J. L. Rubenstone, The thermal oceanographic signal of El Niño reconstructed from a Kiritimati Island coral, *J. Geophys. Res.*, *104*, 13,409–13,421, 1999.

Evans, M. N., A. Kaplan, M. A. Cane, and R. Villalba, Globality and optimality in climate field reconstructions from proxy data, in *Present and Past Inter-Hemispheric Climate Linkages in the Americas and Their Societal Effects*, edited by V. Markgraf, Cambridge Univ. Press, New York, 2000.

Fairbanks, R. G., and R. E. Dodge, Annual periodicity of the $^{18}O/^{16}O$ and $^{13}C/^{12}C$ ratios in the coral *Montastrea annularis*, *Geochim. Cosmochim. Acta*, *43*, 1009–1020, 1979.

Fairbanks, R. G., M. N. Evans, J. L. Rubenstone, R. A. Mortlock, K. Broad, M. D. Moore, and C. D. Charles, Evaluating climate indices and their geochemical proxies measured in corals, *Coral Reefs*, *16*, S93–S100, 1997.

Fritts, H. C., *Reconstructing Large-Scale Climatic Patterns From Tre*

Ring Data: A Diagnostic Analysis, Univ. of Ariz. Press, Tucson, 1991.

Gat, J. R., Oxygen and hydrogen isotopes in the hydrologic cycle, *Ann. Rev. Earth Planet. Sci.*, *24*, 225–262, 1996.

Guilderson, T. P., Tropical Atlantic SSTs over the last 20,000 years: Implications on the mechanism and synchroneity of interhemispheric climate change, Ph.D. thesis, Columbia Univ., New York, 1997.

Heiss, G. A., Coral reefs in the Red Sea: Growth, production and stable isotopes, *Tech. Rep.* 32, GEOMAR, Kiel, Germany, 1994.

Hurrell, J. W., and K. E. Trenberth, Global sea surface temperature analyses: Multiple problems and their implications for climate analysis, modeling and reanalysis, *Bull. Am. Meteorol. Soc.*, *80*, 2661–2678, 1999.

Jones, P. D., R. S. Bradley, and J. Jouzel, *Climatic Variations and Forcing Mechanisms of the Last 2000 Years*, *NATO ASI Ser. I; 41*, 1996.

Jones, P. D., K. R. Briffa, T. P. Barnett, and S. F. B. Tett, High-resolution palaeoclimatic records for the last millennium: Interpretation, integration and comparison with general circulation model control run temperatures, *The Holocene*, *8*, pp. 455–471, 1998.

Kaplan, A., Y. Kushnir, M. A. Cane, and M. B. Blumenthal, Reduced space optimal analysis for historical datasets: 136 years of Atlantic sea surface temperatures, *J. Geophys. Res.*, *102*, 27,835–27,860, 1997.

Kaplan, A., M. A. Cane, Y. Kushnir, A. C. Clement, M. B. Blumenthal, and B. Rajagopalan, Analyses of global sea surface temperature 1856-1991, *J. Geophys. Res.*, *103*, 18,567–18,589, 1998.

Kaplan, A., M. A. Cane, and Y. Kushnir, Reduced space approach to the optimal analysis of historical marine observations: Accomplishments, difficulties, and prospects, paper presented at CLIMAR 99, WMO Workshop on Advances in Marine Climatology, World Meteorol. Org., Vancouver, Canada, 1999.

Linsley, B. K., R. B. Dunbar, G. M. Wellington, and D. A. Mucciarone, A coral-based reconstruction of Intertropical Convergence Zone variability over Central America since 1707, *J. Geophys. Res.*, *99*, 9977–9994, 1994.

Martinson, D. G., K. Bryan, M. Ghil, M. M. Hall, T. R. Karl, E. S. Sarachik, S. Sorooshian, and L. Talley (Eds.), *Natural Climate Variability on Decade-to-Century Time Scales*, Natl. Acad. of Sci., Washington, D.C., 1995.

McConnaughey, T., ^{13}C and ^{18}O isotopic disequilibrium in biological carbonates, I, Patterns, *Geochim. Cosmochim. Acta*, *53*, 151–162, 1989.

McCrea, J. M., On the isotopic chemistry of carbonates and a paleotemperature scale, *J. Chem. Phys.*, *18*, 849–857, 1950.

McCulloch, M. T., M. K. Gagan, G. E. Mortimer, A. R. Chivas, and P. J. Isdale, A high-resolution Sr/Ca and $\delta^{18}O$ coral record from the Great Barrier Reef, Australia, and the 1982-1983 El Niño, *Geochim. Cosmochim. Acta*, *58*, 2747–2754, 1994.

Moore, M. D., and C. D. Charles, Interdecadal temperature variability of the Pacific western boundary observed in a coral from the Indonesian Seaway, in *EOS, Trans. AGU, 79*(17), Spring Meet. Suppl., S178, 1998.

Parker, D. E., P. D. Jones, C. K. Folland, and A. Bevan, Interdecadal changes of surface temperature since the late nineteenth century, *J. Geophys. Res.*, *99*, 14,373–14,399, 1994.

Patzöld, J., Growth rhythms recorded in stable isotopes and density bands in the reef coral *Porites lobata* (Cebu, Phillipines), *Coral Reefs*, *3*, 87–90, 1984.

Preisendorfer, R. W., *Principal Component Analysis in Meteorology and Oceanography*, Elsevier Sci., New York, 1988.

Quinn, T. M., F. W. Taylor, and T. J. Crowley, A 173 year stable isotope record from a tropical South Pacific coral, *Quat. Sci. Rev.*, *12*, 407–418, 1993.

Quinn, T. M., T. J. Crowley, and F. W. Taylor, New stable isotope results from a 173-year coral from Espiritu Santo, vanuatu, *Geophys. Res. Lett.*, *23*, 3413–3416, 1996.

Quinn, T. M., T. M. Crowley, F. W. Taylor, C. Henin, P. Joannot, and Y. Join, A multicentury stable isotope record from a New Caledonia coral: Interannual and decadal sea surface temperature variability in the southwest Pacific since 1657 A.D., *Paleoceanography*, *13*, 412–426, 1998.

Ropelewski,
C. F., and M. S. Halpert, Global and regional scale precipitation patterns associated with the El Niño/Southern Oscillation., *Mon. Weather Rev.*, *114*, 2352–2362, 1987.

Shen, G. T., J. E. Cole, D. W. Lea, L. J. Linn, T. A. McConnaughey, and R. G. Fairbanks, Surface ocean variability at Galápagos from 1936-1982: Calibration of geochemical tracers in corals, *Paleoceanography*, *7*, 563–588, 1992.

Sokal, R. R., and F. J. Rohlf, *Biometry: The Principles and Practice of Statistics in Biological Research*, 3rd ed., W. H. Freeman, New York, 1995.

Trenberth, K. E., Some effects of finite sample size and persistence on meteorological statistics, part I, Autocorrelations, *Mon. Weather Rev.*, *112*, 2359–2379, 1984.

Tudhope, A. W., G. B. Shimmield, C. P. Chilcott, M. Jebb, A. E. Fallick, and A. N. Dalgleish, Recent changes in climate in the far western equatorial Pacific and their relationship to the Southern Oscillation; oxygen isotope records from massive corals, *Earth Planet. Sci. Lett.*, *136*, 575–590, 1995.

Villalba, R., R. D. D'Arrigo, E. R. Cook, G. Wiles, and G. C. Jacoby, Decadal-scale climatic variability along the extra-tropical western coast of the Americas over past centuries inferred from tree-ring records, in *Present and Past Interhemispheric Climate Linkages in the Americas and their Societal Effects*, edited by V. Markgraf, Cambridge Univ. Press, New York, 1999.

Weber, J. N., and P. M. J. Woodhead, Temperature dependence of Oxygen-18 concentration in reef coral carbonates, *J. Geophys. Res.*, *77*, 463–473, 1972.

Wellington, G. M., R. B. Dunbar, and G. Merlen, Calibration of stable oxygen isotope signatures in Galápagos corals, *Paleoceanography*, *11*, 467–480, 1996.

Zhang, Y., J. M. Wallace, and D. S. Battisti, ENSO-like interdecadal variability: 1900-93, *J. Clim.*, *10*, 1004–1020, 1997.

M.A. Cane and A. Kaplan, Lamont-Doherty Earth Observatory, Oceanography 103, Route 9W, Palisades, NY 10964.

M.N. Evans, Harvard University, Department of Earth and Planetary Sciences, 20 Oxford St., Cambridge, MA 02138. (mevans@fas.harvard.edu)

(Received January 11, 2000;
accepted February 18, 2000.)